European Journal of Medicinal Chemistry 67 (2013) 359–366

Contents lists available at SciVerse ScienceDirect

European Journal of Medicinal Chemistry

journal homepage: http://www.elsevier.com/locate/ejmech

Original article

Synthetic polyamines activating autophagy: Effects on cancer cell death

Anna Minarini [a], Maddalena Zini [b], Andrea Milelli [c], Vincenzo Tumiatti [c], Chiara Marchetti [a], Benedetta Nicolini [b], Mirella Falconi [b], Giovanna Farruggia [a], Concettina Cappadone [a], Claudio Stefanelli [c,*]

[a] Department of Pharmacy and Biotechnology, University of Bologna, 40126 Bologna, Italy
[b] Department of Biomedical and Neuromotor Sciences, University of Bologna, 40126 Bologna, Italy
[c] Department for Life Quality Studies, University of Bologna, Rimini campus, 47921 Rimini, Italy

ARTICLE INFO

Article history:
Received 31 January 2013
Received in revised form
20 June 2013
Accepted 21 June 2013
Available online 1 July 2013

Keywords:
Polyamine analogs
Autophagy
Oxidative stress
Cancer therapy

ABSTRACT

The ability of symmetrically substituted long chain polymethylene tetramines, methoctramine (**1**) and its analogs **2**–**4** to kill cancer cells was studied. We found that an elevated cytotoxicity was correlated with a 12 methylene chain length separating the inner amine functions (6-12-6 carbon backbone), together with the introduction of diphenylethyl moieties on the terminal nitrogen atoms (compound **4**) of a tetramine backbone. Compound **4** triggered dissipation of mitochondrial transmembrane potential and increased intracellular peroxide levels, leading to a caspase-independent HeLa cell death associated with a rapid activation of autophagy. The antioxidant *N*-acetylcysteine inhibited cell death and activation of autophagy, indicating a link between oxidative stress and autophagy. Autophagy was rapidly triggered even by tetramines **2** and **3**, indicating that is related to their polyamine structure. Autophagy did not protect HeLa cells against cytotoxicity elicited by compound **4**. The present study shows that, by modifications of the methoctramine structure, it is possible to design polyamine derivatives highly cytotoxic against tumor cells and that the appropriate design of molecules bearing polyamine-like structures leads to powerful inducers of autophagy.

1. Introduction

Research in the polyamine field continues to have a great potential for the development of novel therapeutic agents against proliferative disorders. As pointed out by Casero and Woster [1], in the course of the last thirty years the research has progressively moved from the search of specific inhibitors acting on enzymes of polyamine metabolism toward the design of polyamine analogs acting as polyamine mimetics or polyamine antimetabolites. Polyamines are involved in multiple cellular processes, including those linked to cell growth and survival such as cell cycle, apoptosis and autophagy [2–4]. For this reason, polyamines have a central role in cancer development [5] and by interfering with polyamine metabolism and functions it is possible to affect cancer cell proliferation at different levels [6–8].

The polycationic structure of alkylpolyamines, together with the lipophilic polymethylene chains, allow them to interact with a variety of cellular targets so that the polyamine structure may represent an universal template for the recognition of many receptor sites [9,10]. In fact, it was verified that it is possible to modulate both affinity and selectivity for diverse receptor systems by inserting different groups onto a polymethylene backbone, as well as appropriate spacers separating the amine functions [11,12]. Methoctramine (**1**), for example, represents the prototype of polymethylene tetramines acting as muscarinic receptor competitive antagonists [13]. Regarding the muscarinic receptor activity, a huge study of structure–activity relationships on **1**-derivatives was performed, in particular, by modifying the methylene chain length between the inner nitrogen atoms [9]. Only recently we have reported that the cytotoxicity of **1** and its analogs is strongly correlated to the methylene chain length separating the inner nitrogen atoms, increasing from 5 to 12 units [14], suggesting that cytotoxicity of these

Abbreviations: AO, acridine orange; Atg5, autophagy gene 5; AVOs, acidic vesicular organelles; DCFDA, dichlorofluoresceine diacetate; DFMO, α-difluoromethylornithine; DENSPM, N^1,N^{11}-diethylnorspermine; DiOC6, 3,3′-dihexyloxacarbocyanine iodide; DMSO, dimethylsulphoxide; NAC, *N*-acetylcysteine; TEM, transmission electron microscopy.

* Corresponding author. Tel.: +39 51 2091207; fax: +39 51 2091224.
E-mail address: claudio.stefanelli@unibo.it (C. Stefanelli).

0223-5234/$ – see front matter © 2013 Elsevier Masson SAS. All rights reserved.
http://dx.doi.org/10.1016/j.ejmech.2013.06.044

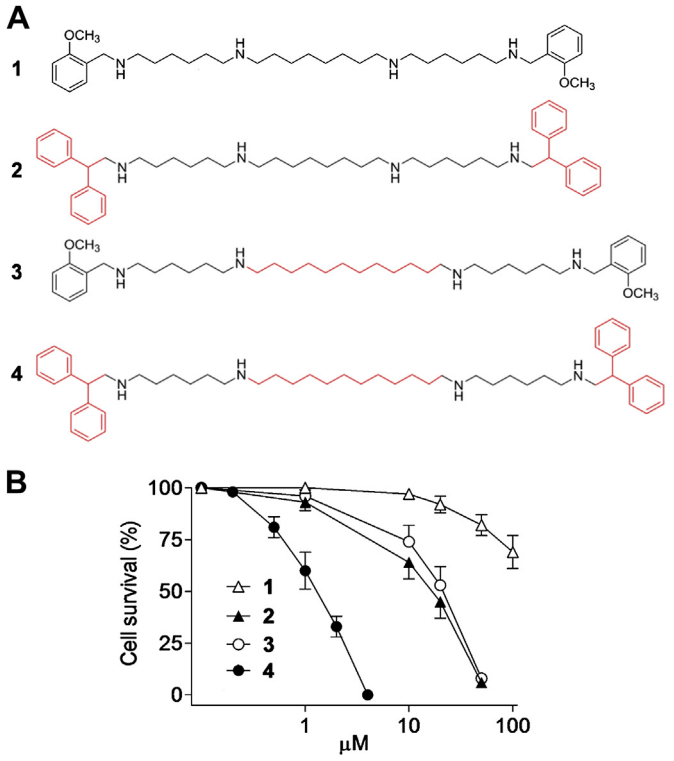

Fig. 1. Structure and cytotoxicity of the symmetric polymethylene tetramines **1**–**4**. (A) Chemical structure of compounds **1**–**4**; in red the structural differences with respect to compound **1** (methoctramine). (B) Induction of cell death by compounds **1**–**4** in HL60 cells incubated for 24 h with increasing concentrations of the indicated compounds. The figure reports means ± S.E.M. of three determinations. (For interpretation of the references to color in this figure legend, the reader is referred to the web version of this article.)

molecules should be associated to lipophilicity and that appropriate tetramine backbone can be used for the development of anticancer drugs. In addition, in preliminary experiments we observed an increased toxic effect, in comparison to **1**, of compound **2**, obtained by replacing the terminal 2-methoxybenzyl groups of **1** with the more lipophilic diphenylethyl moieties. This last chemical feature was already reported to confer antitumor activity (μM range) when mounted on terminal nitrogen atoms of spermine, norspermine and spermidine [1]. For this reason, we thought of interest to design and synthesize a new polymethylene tetramine (**4**) bearing an inner 12 methylene chain length and diphenylethyl moieties on terminal nitrogens, with the aim to investigate a possible additive effect of these two chemical features that we found to increase cytotoxicity. Very recently we found that compounds with these chemical features act as potent *N*-methyl-D-aspartate (NMDA) receptor channel blockers [15].

In the present work we went deeply inside to the mechanism of cytotoxicity elicited by symmetrically substituted tetramines **1**–**4**. Interestingly, the investigation of the mechanisms of cell death, revealed that the cytotoxic effect of **1**-derivatives against cancer cells is associated with activation of autophagy.

2. Results and discussion

2.1. Chemistry

Fig. 1A shows the structure of the tetramine compounds used in this study, i.e, methoctramine (**1**); the derivative in which the 2-methoxybenzyl groups of **1** were replaced with a diphenylethyl moieties (**2**); the **1**-derivative in which the octamethylene spacer separating the inner amine functions was replaced with a 12 methylene chain (**3**); the newly synthesized derivative combining both modifications, the inner 12 methylene chain and the terminal diphenylethyl moieties (**4**). Compounds **1**–**3** have been synthesized as previously reported [16–18]. Compound **4** was synthesized following the procedure reported in Scheme 1 and was characterized by IR, ^{1}H NMR, ^{13}C NMR, mass spectra, and elemental analysis. Briefly, intermediate **5** was obtained by reacting *N*-[(benzyloxy)carbonyl]-6-aminocaproic acid with 1,12-diaminododecane; removal of the *N*-(benzyloxy)carbonyl group by acidic hydrolysis gave diamine diamide **6**, which was treated with 2,2-diphenylacetyl chloride to furnish derivative **7**; reduction with borane *N*-ethyl-*N*-isopropylaniline complex (BACH-EI) in dry THF [19] led to the tetraamine compound **4**.

2.2. Cytotoxicity

The cytotoxic activities of **1** and its analogs **2**–**4** were evaluated against HeLa cervical carcinoma cells, incubated for 24 h in the presence of increasing concentration of the analogs (Fig. 1B). Compounds **2** and **3** elicited a similar moderate toxicity, however, when their structural determinants of toxicity were combined as in compound **4**, the effect was synergistic and cytotoxicity was largely increased. Cytotoxicity of **1**–**4** was also examined against non-cancerous cells, such as immortalized human chondrocytes

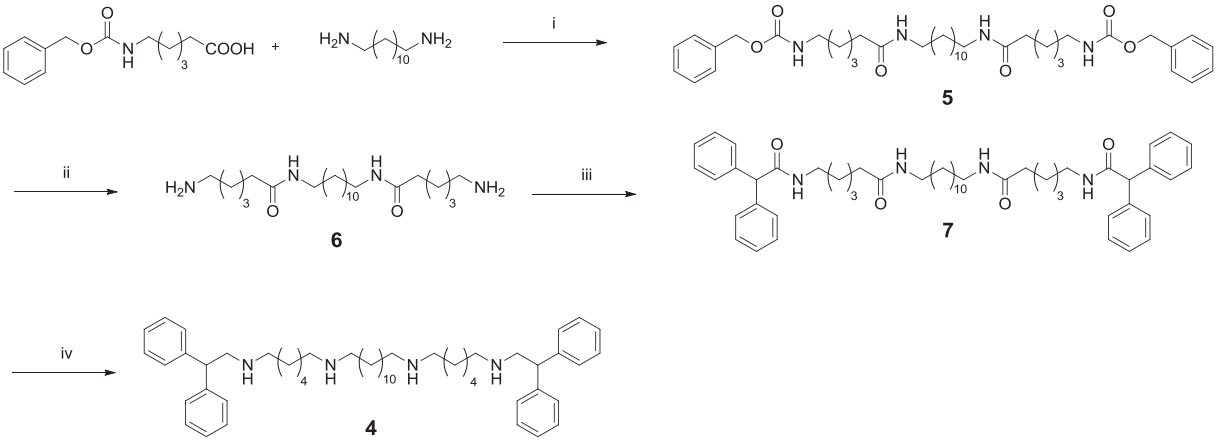

Scheme 1. Procedure for the preparation of compound **4**. (i) EtOCOCl, NEt_3, dioxane, room temp., 18 h, 84% yield; (ii) a) HBr 33% in CH_3COOH, room temp., 4 h, quantitative yield; b) 2 N NaOH, $CHCl_3$, 14 h; (iii) 2,2-diphenylacetyl chloride, NEt_3, CH_2Cl_2, room temp., overnight, 20% yield; (iv) BACH-EI, diglyme, reflux, 9 h, 36% yield.

Table 1
IC_{50} values of tetramines against different cells. The data were obtained after treating the cells with increasing concentration of the indicated compound for 24 h. Data are means ± S.E.M. of three replicates.

Compound	IC_{50} (μM)		
	HeLa	C28/I2 chondrocytes	Rat thymocytes
1 (Methoctramine)	>100	>100	>100
2	18 ± 4	60 ± 5	82 ± 6
3	21 ± 4	77 ± 6	>100
4	1.6 ± 0.3	4.3 ± 0.3	6.8 ± 0.5

C-28/I2 and primary rat thymocytes (Table 1). In these non-cancerous cells, compounds **1**–**3** exhibited a very low cytotoxicity and the effect of compound **4** was lower respect to HeLa carcinoma cells.

The IC_{50} values of **4** against seven different cancer cell lines, calculated in experiments similar to that depicted in Fig. 1B, were in the low micromolar range at 24 h and fell in the high nanomolar range at 48 h (Table 2). Osteosarcoma cells apparently exhibited the higher sensitivity to **4**, being p53-null Saos-2 the most sensitive cells among those tested.

2.3. Mechanisms associated with cytotoxicity

The mechanisms involved in cell death were investigated in HeLa cells. We have previously shown that the toxicity of compound **3** is linked to cellular internalization and induction of oxidative stress [14]. In order to detect whether oxidative stress is also involved in the cytotoxic effect of compound **4** and if it is associated to mitochondrial events, we investigated the effects of **4** on the mitochondrial membrane potential (ΔΨm), measured in intact cells by using the fluorescent probe 3,3′-dihexyloxacarbocyanine iodide (DiOC6). This compound can accumulate and aggregate into mitochondria, leading to a green fluorescence. Following Ψm collapse, DiOC6 no longer enters mitochondria, resulting in a decrease in green fluorescence. Fig. 2A shows that a 4 h treatment with **4** caused in the cell population a decrease of more than 50% in the mean DiOC6 signal (from channel 216 to channel 98), indicating a marked disruption of ΔΨm. Since the depolarization of the mitochondrial membrane is associated with mitochondrial production of ROS, we evaluated the intracellular oxidative stress elicited by dichlorofluoresceine diacetate (DCFDA), that is hydrolyzed by intracellular esterases to dichlorohydrofluorescein which is oxidized to the highly fluorescent dichlorofluorescein (DCF) by cellular peroxides. The treatment of HeLa cells with compound **4** caused a significant increase in DCF fluorescence in the cell population (from channel 41 to channel 77, Fig. 2B), indicating increased peroxide production. The antioxidant *N*-acetylcysteine (NAC) protected the cells from **4**-induced cell death, showing that oxidative stress is involved in the pathway leading to cell death directly or by influencing the redox status of the cell (Fig. 2C).

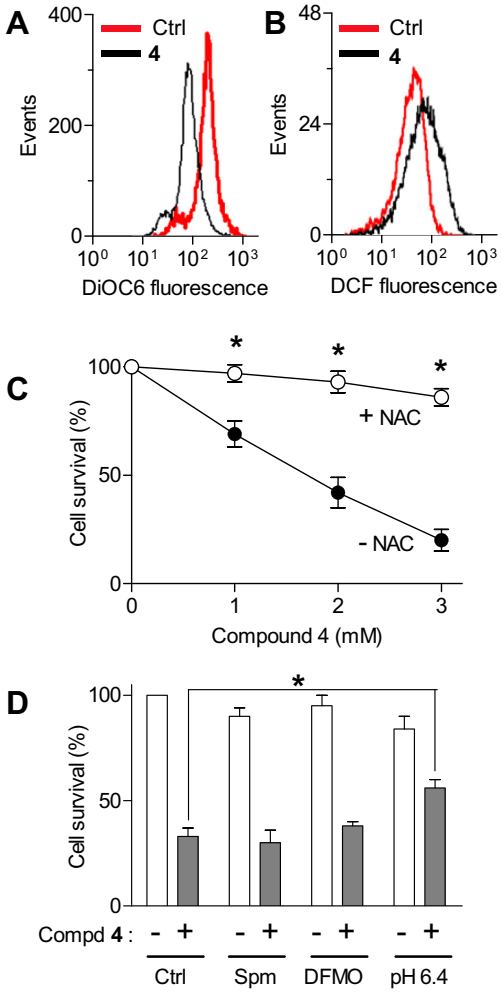

Fig. 2. Characteristics of cell death triggered by compound **4** in HeLa cells. (A) Change in mitochondrial membrane potential as estimated from DiOC6 fluorescence in cells treated for 3 h with DMSO (control) or 2 μM **4**. ΔΨm collapse in **4**-treated cells is evidenced by a decrease in DiOC6 fluorescence histograms. (B) Histogram profiles of control and **4**-treated cells upon DCFDA staining. The increase in the mean fluorescence intensity (DCF-positive cells) in cells incubated 3 h in the presence of 2 μM **4**, indicates an increase in intracellular peroxides. (C) Cell viability was measured in cells treated for 24 h with the indicated concentration of compound **4** in the absence or presence of 5 mM NAC. Results are means ± S.E.M. of triplicate determinations, $^*P < 0.05$ vs. cells incubated in the absence of NAC. (D) Cell survival was measured in cells incubated for 24 h in the absence or presence of compound **4** (2 μM) together with treatments that could affect its cellular uptake: 0.5 mM spermine (together with 1 mM aminoguanidine to inhibit serum amine oxidases in the medium); 0.1 mM DFMO (48 h pretreatment); incubation in a medium in which the pH was adjusted to 6.4 with HCl. Results are mean ± S.E.M. of triplicate determinations, $^*P < 0.05$ vs. control cells.

The effect of antioxidants has been examined rarely in the literature dealing with polyamine analogs. However, a protective effect of NAC was reported in the case of anticancer agents, such as N^1,N^{11}-diethylnorspermine (DENSPM) [20], mononaphthalimide-spermidine [21], and polyamine-containing naphthalene diimides [22]. This protective role of antioxidants needs to be taken in account in evaluating either the therapeutic potential or the strategy to decrease toxicity in normal non-tumor cells.

Cytotoxicity of **4** was not influenced by addition to the medium of spermine or by 48 h pre-treatment with the polyamine synthesis inhibitor, α-difluoromethylornithine (DFMO), used in order to obtain polyamine depletion (Fig. 2D), suggesting that the polyamine transport system is not significantly involved in the action of

Table 2
IC_{50} values of compound **4** against cancer cell lines. The data were obtained by treating the cells with increasing concentration of compound **4** for the indicated time. Results are means ± S.E.M. of three to four replicates.

Cell line	IC_{50} (μM)	
	24 h	48 h
Saos-2 osteosarcoma	0.9 ± 0.1	0.3 ± 0.1
U2OS osteosarcoma	1.1 ± 0.2	0.4 ± 0.1
HeLa cervical carcinoma	1.6 ± 0.3	0.6 ± 0.1
HL60 myeloid leukemia	1.9 ± 0.2	0.7 ± 0.1
LOVO colorectal adenocarcinoma	2.0 ± 0.3	0.8 ± 0.2
HT29 colon cancer	2.4 ± 0.2	1.1 ± 0.3
SHSY-5Y neuroblastoma	2.8 ± 0.4	0.9 ± 0.2

4. In fact, spermine should decrease **4** internalization by competition, whereas DFMO, an inhibitor of ornithine decarboxylase, should increase the entry of **4**, since polyamine depletion activates the transport system [23]. Compound **4** could enter by simple diffusion [24] and/or by endocytosis [25], that may be facilitated by the lipophilicity of the long polymethylene chains and of the terminal groups. Actually, cell survival of **4**-treated cells was significantly increased when the cells were incubated in a medium in which the pH was adjusted to 6.4 with HCl, instead of 7.2, in order to increase the positive net charge of nitrogen atoms that is expected to decrease the cross of the plasma membrane by diffusion. Altogether, these data suggest a picture in which compound **4** enters into the cell by diffusion and triggers an oxidative insult, possibly by interference with mitochondrial function.

2.4. Compound *4* rapidly activates autophagy

Mitochondrial damage and oxidant production are often associated with activation of apoptosis, hence we determined the activation of caspases acting on the substrate Asp-Glu-Val-Asp (DEVD), i.e. mainly effector caspases 3 and 7, whose activation is characteristic of apoptotic cell death [26]. The polyamine analog DENSPM was used as positive control [20]. The cells were treated for 24 h with 25 μM DENSPM or 2 μM compound **4** (these treatments reduced cell survival by 50–70%). DENSPM significantly increased caspase activity (Fig. 3A), as expected. On the contrary, compound **4** did not activate caspases. Furthermore, following DAPI staining for nuclear morphology, in **4**-treated cells it was not possible to detect the nuclear characteristics of apoptosis [27], i.e. chromatin condensation, nuclear fragmentation and/or condensation (not shown). We can conclude that compound **4** kills HeLa cells in a caspase-independent manner. Actually, cell survival was not affected by the caspase inhibitor Z-VADfmk (Fig. 3B). Further, the effect of **4** was not influenced by necrostatin-1 that can discriminate necroptosis, a different form of cell death [28].

Autophagy is another emerging process that may be associated to a programmed form of cell death and can be activated by tumor chemotherapy [28–30]. The natural polyamine spermidine reportedly activates autophagy [31], so we verified whether cell death induced by the tetramine compounds used in this study was linked to autophagy. Transmission electron microscopy (TEM) analysis of **4**-treated HeLa cells (Fig. 3C) demonstrated the presence of several vacuoles in the cytoplasm, often containing high-electron-density substances. At higher magnification these vacuoles showed organic material inside, characteristic of the autophagocytosis process during autophagy (Fig. 3C, images III–V).

Development of acidic vesicular organelles (AVOs) is a typical feature of autophagy, that indicates the maturation of autophagosomes. Acridine orange (AO) is a marker of AVOs, that fluoresces green in the whole cell but it is taken up in acidic compartments (mainly late autophagosomes), where it fluoresces red. HeLa cells were treated with **4** (2 μM) and incubated for various times, afterward the cells were stained with AO and analyzed by fluorescence microscopy. As soon as 3 h, it resulted evident the appearance of orange–red fluorescence in a large number of cells, indicative of the formation of acidic vesicles (Fig. 4A). The formation of AVOs was inhibited when the HeLa cells were pretreated with the antioxidant NAC.

To further obtain a biochemical evidence for autophagy, we determined the change in the expression level of LC3 protein. LC3 exists in two forms, an 18-kDa cytosolic protein (LC3-I) that during autophagy is processed to a membrane-bound 16-kDa form conjugated with phosphatidylethanolamine (LC3-II). The lipidated LC3-II increases following activation of the autophagic pathway by conversion from LC3-I, and is a hallmark of autophagy [32]. We

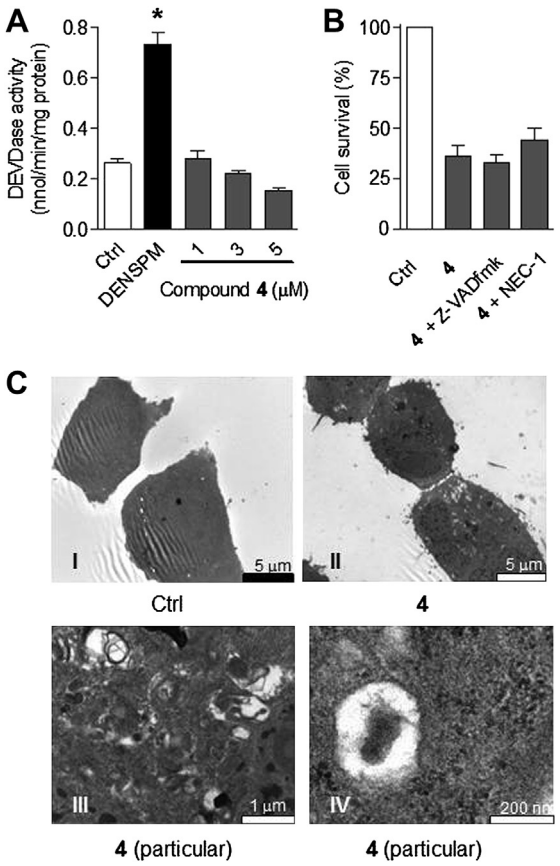

Fig. 3. Compound **4** does not trigger apoptosis, but activates autophagy in HeLa cells. (A) Caspase (DEVDase) activity was measured in cells treated for 24 h with 25 μM DENSPM or the indicated concentration of compounds **4**. Data are means ± S.E.M. of three replicates, $^{*}P < 0.05$ vs. control cells. (B) Cytotoxicity of **4** was determined in cells pretreated for 2 h with Z-VADfmk (50 μM), or with necrostatin-1 (NEC-1, 20 μM). Data are means ± S.E.M. of three determinations. (C) Representative transmission electron micrographs showing the ultrastructure of control HeLa cells (panel I, bar 5 μm) and of cells treated with 2 μM **4** for 24 h (panels II–IV). Many vacuoles are detectable in the cytoplasm of **4**-treated cells (II, bar 5 μm). Higher magnification of vacuoles reveals that organic material is detectable inside (III, bar 1 μm). Panel IV (bar 200 nm) shows a mitochondrion entrapped inside a vacuole.

examined LC3-I and LC3-II levels by Western blotting. As shown in Fig. 4B, LC3-I was largely converted into LC3-II, whose level was greatly increased during 3 h following the treatment with compound **4**. Again, NAC prevented the processing of LC3-I. LC3 processing was evident even in the presence of bafilomycin A (not shown). This observation, together with the formation of AVOs, indicates the persistence of the autophagic flux. Altogether, these data show that **4** rapidly activated autophagy in HeLa cells, apparently as a consequence of an oxidative event, since it is blocked by NAC.

Autophagy represents a double-edged sword for cell survival because it acts as a prosurvival mechanism, mainly in adverse conditions of cellular stress, but it is generally thought that the process has a self-limiting character and leads to autophagic cell death when excessive [29,30]. However, this view is not universally accepted. Other researchers hypothesized that autophagy is only a protective mechanism and not cause of cell death [33], so the precise role of autophagy in cell death is still debated [34]. Actually, several reports highlight a tumor-killing role of autophagy following anticancer treatment or, at the opposite, a protective role of autophagy against chemotherapy [28–30]. So we wondered how **4**-triggered autophagy can affect cell death. To address this

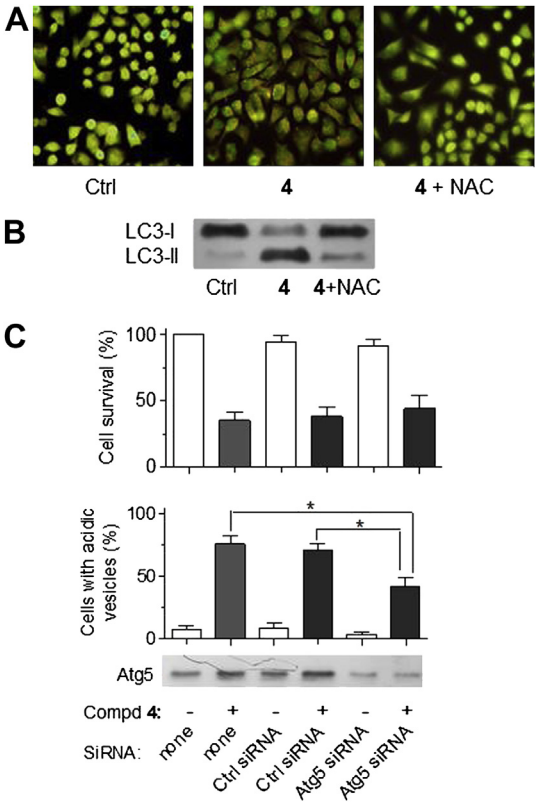

Fig. 4. Characteristics of autophagy activated by compound **4** in HeLa cells. (A) Immunofluorescence microscopy of acridine orange-stained HeLa cells treated for 3 h with DMSO (ctrl) or 2 μM **4**. Increase in number of cells with AO accumulating acidic vesicular organelles (orange–red fluorescence) in **4**-treated cells was inhibited by pretreatment (2 h) with 5 mM NAC. Similar results were observed in two independent experiments. (B) Western blot analysis of LC3-I and LC3-II expression in cells treated with 2 μM **4** for 3 h in the presence or absence of 5 mM NAC. The image is representative of multiple independent experiments. (C) Untransfected cells and cells transfected with Atg5-siRNA or control siRNA were incubated for 24 h in the absence or presence of 2 μM **4**. The extent of cell death and the accumulation of acidic vescicles were then measured. Values are means ± S.E.M. of triplicate determinations, $^{*}P < 0.05$. The blot shows Atg5 expression and is representative of 3 experiments.

question we thought to perform experiments in the presence of autophagy inhibitors. Experiments done by using pharmacological inhibitors of signal transduction pathways involved in autophagy activation, such as inhibitors of class III phosphoinositide 3′-kinase (PI3K) like 3-methyladenine, are widely reported in literature. Since in our assays we observed that these compounds were highly toxic by themselves to HeLa cells, hampering their use to study cell survival, a siRNA approach was used. The cells were transfected with a siRNA targeting Atg5, characterized as part of an ubiquitin-like conjugation systems specifically required for autophagy [35], whose silencing is frequently used to inhibit autophagy. The cells transfected with Atg5 siRNA showed a level of the Atg5 protein reduced of about 60%, associated with a significant inhibition of acidic vesicles accumulation after treatment with **4**, when compared with cells transfected with control siRNA (Fig. 4C). Inhibition of autophagy apparently resulted in a slight attenuation of the cytotoxic effect of compound **4**, but the difference was not statistically significant ($P = 0.12$). Our results suggest that autophagy activation is not the main cause of cell death but, on the other hand, autophagy does not ever protect HeLa cells from **4**-induced cytotoxicity. We suggest that autophagy is activated as a defense mechanism in response to the oxidative insult triggered by **4**, but the effect of **4** is so rapid and powerful that equally leads to cell death.

2.5. Autophagy is activated by other polyamine derivatives

Fig. 5A shows that autophagy was rapidly activated within 3 h even by compounds **2** and **3** at toxic concentrations (20 μM), indicating that induction of autophagy is a common feature of cytotoxic **1**-derivatives and seems to be associated with their polyamine structure and not with the character of terminal groups. Also the natural polyamine spermidine has been reported to activate autophagy [31]. In order to compare the effect of spermidine with that of compound **4**, we treated HeLa cells with increasing concentrations of spermidine: to observe LC3-I processing, it was necessary to incubate the cells for at least 24 h with a very high spermidine concentration (8 mM), that elicits toxic effect [36]. On the other hand, the polyamine analog DENSPM caused a very limited LC3-I processing, even at toxic levels. The experiment depicted in Fig. 5B compares the effect of polyamine compounds at concentrations that reduce cell survival to 30–50% on LC3-I processing.

To date, in the field of polyamine analogs, autophagy activation was reported only in the case of an anticancer–norspermine conjugate in which the unique role of the norspermine moiety was to facilitate the import of the cytotoxic part of the molecule into the cell by means of the polyamines transport system [37]. Differently, our data show that the ability of the cytotoxic disubstituted long chain polymethylene tetramines to activate autophagy is correlated primarily to their polyamine backbone rather than to the terminal

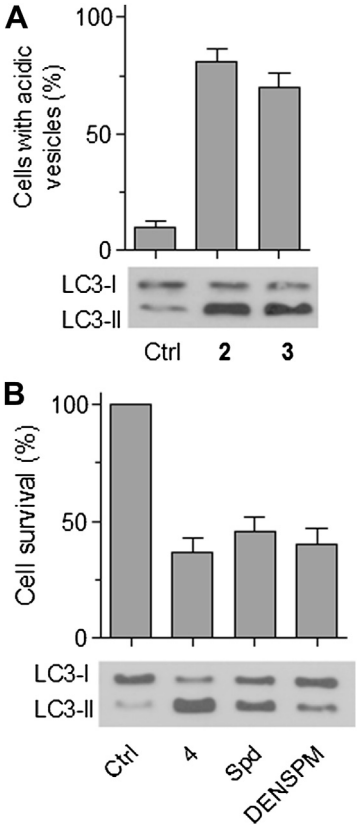

Fig. 5. Activation of autophagy by polyamine compounds in HeLa cells. (A) The cells were incubated for 3 h in the presence of compounds **2** or **3** (20 μM) afterward, accumulation of acidic vesicles and LC3 expression/processing were examined. Values are means ± S.E.M. of triplicate measurements. (B) HeLa cells were incubated for 24 h in the presence of polyamine compounds at concentrations that reduced cell survival by 50–70%: compounds **4** (2 μM) or spermidine (Spd, 8 mM) or DENSPM (25 μM); cell survival and LC3 expression/processing were then examined. Values are as means ± S.EM. of three determinations.

aromatic groups. Possibly, the main role of the terminal substituents and the methylene chain length of the compounds used in the present study is to facilitate the internalization and the localization of the molecule inside the cell.

2.6. Conclusions

In conclusion, we have shown that, by appropriate modifications of the methoctramine structure, it is possible to design polyamine derivatives, highly cytotoxic against tumor cells. The most potent compound **4** triggers an oxidative insult leading to a caspase-independent form of cell death associated with the rapid onset of autophagy. Autophagy is a process for recycling cellular constituents that can be associated with either cell death or cell survival and is implicated in several pathological and physiological processes [38]. In our opinion the most relevant finding of this work is that the design of polyamine-like structures, bearing appropriate molecular features, leads to powerful inducers of autophagy.

3. Materials and methods

3.1. Chemistry

All the synthesized compounds have a purity of at least 95% determined by elemental analysis. Uncorrected melting point was taken in glass capillary tubes on a Buchi SMP-20 apparatus. ESI-MS spectra were recorded on Perkin Elmer 297 and Waters ZQ 4000. ^{1}H NMR and ^{13}C NMR were recorded on Varian VRX 200 and 400 instruments. Chemical shifts are reported in parts per million (ppm) relative to peak of tetramethylsilane (TMS) and spin multiplicities are given as s (singlet), br s (broad singlet), d (doublet), t (triplet), q (quartet) or m (multiplet). IR spectral data were consistent with the assigned structures. The elemental analysis was performed with Perkin Elmer elemental analyzer 2400 CHN. From all new compounds satisfactory elemental analyses were obtained, confirming >95% purity. Chromatographic separations were performed on silica gel columns by flash (Kieselgel 40, 0.040 e 0.063 mm, Merck) column chromatography. Reactions were followed by thin layer chromatography (TLC) on Merck (0.25 mm) glass-packed precoated silica gel plates (60 F254) and then visualized in an iodine chamber or with a UV lamp.

Compounds **1**–**3** have been synthesized as previously reported [16,17]. The newly designed compound **4** was synthesized following the general procedure developed by our research group as follows (see Scheme 1):

3.1.1. Synthesis of dibenzyl ((dodecane-1,12-diylbis(azanediyl)) bis(6-oxohexane-6,1-diyl))dicarbamate (**5**)

Ethyl chloroformate (1.56 ml, 16.4 mmol) in dry dioxane (50 ml) was added dropwise to a stirred and cooled (0 °C) solution of 6-(((benzyloxy)carbonyl)amino)hexanoic acid (4.35 g, 16.4 mmol) and Et_3N (2.29 ml, 16.4 mmol) in dioxane (30 ml), followed after standing for 30 min by the addition of 1,12-diaminododecane (1.64 g, 8.2 mmol) in dioxane (20 ml). After the mixture was stirred at room temperature for 18 h, it was poured into water (100 ml), and the white solid was filtered, washed with $NaHCO_3$ saturated solution, HCl 2 N, *i*-PrOH, Et_2O and crystallized from DMSO to give the intermediate **5** as white solid. 84% yield, mp 158–161 °C, ^{1}H NMR (200 MHz, DMSO) δ 1.22–1.45 (m, 32H), 2.00 (t, 4H, $J = 7.2$), 2.94–2.99 (m, 8H), 4.98 (s, 4H), 7.31–7.34 (m, 8H), 8.66–8.68 (m, 2H).

3.1.2. Synthesis of N,N′-(dodecane-1,12-diyl)bis(6-aminohexanamide) (**6**)

solution of 30% HBr in acetic acid (43 ml) was added to a solution of **5** (5.13 g, 7.1 mmol) in acetic acid (70 ml), and the resulting mixture was stirred for 4 h at room temperature. Ether (300 ml) was then added, yielding a solid, which was filtered, washed with ether (3 × 20 ml) and crystallized from EtOH/*i*-PrOH to a white solid. The hydrobromide salt was dissolved in water (30 ml) and the solution was made basic with 2 N NaOH (40 ml). The precipitated product was separated by continuous extraction with $CHCl_3$ (200 ml) for 14 h. The organic phase was dried and evaporated to give compound **6** in quantitative yield, mp 199–202 °C, ^{1}H NMR (200 MHz, CD_3OD) δ 1.32–1.49 (m, 24H), 1.64–1.70 (m, 8H), 2.23 (t, 4H, $J = 7.2$), 2.95 (t, 4H, $J = 7.5$), 3.17 (t, 4H, $J = 6.7$).

3.1.3. Synthesis of N,N′-(dodecane-1,12-diyl)bis(6-(2,2-diphenylacetamido)hexanamide) (**7**)

6 (500 mg, 1.17 mmol) in dry CH_2Cl_2 (10 ml) was added dropwise to a stirred and cooled (0 °C) solution of 2,2-diphenylacetyl chloride (590 mg, 2.6 mmol) and Et_3N (0.49 ml) in dry CH_2Cl_2 (20 ml). The mixture was stirred at room temperature overnight and then washed with water and $NaHCO_3$ saturated solution. After the evaporation of the solvent, the crude material was purified by flash chromatography using as eluent a mixture of CH_2Cl_2/MeOH (9:1). 20% yield, ^{1}H NMR (200 MHz, DMSO) δ 1.22–1.34 (m, 18H), 1.41–1.48 (m, 14H), 1.99 (t, 4H, $J = 7.4$), 2.94–3.06 (m, 8H), 4.90 (s, 2H), 7.16–7.26 (m, 16H), 7.67–7.72 (m, 2H), 8.21–8.27 (m, 2H).

3.1.4. Synthesis of N,N′-(dodecane-1,12-diyl)bis(N^6-(2,2-diphenylethyl)hexane-1,6-diamine) (**4**)

A solution of 2 M BACH-EI in THF (1.16 ml) was added dropwise to a room temperature solution of **7** (237 mg, 2.9 mmol) in dry diglyme (10 ml) under a stream of dry nitrogen. When the addition was completed, the reaction mixture was heated at reflux temperature for 5 h. After cooling at room temperature, excess borane was destroyed by cautious dropwise addition of water (12 ml) and 6 N HCl (12 ml). The resulting mixture was then heated at reflux temperature for 4 h. After solvent evaporation, the crude product was washed with Et_2O/EtOH (5:1), filtered and the solid was purified by flash chromatography using as eluent a mixture of $CHCl_3$/MeOH/aqueous ammonia solution 33% (from 8:2:0.05 to 7:3:0.4). 36% yield; ^{1}H NMR (200 MHz, CD_3OD) δ 1.28–1.41 (m, 24H), 1.65–1.77 (m, 12H), 2.95–3.01 (m, 8H), 3.03–3.07 (m, 4H), 3.77 (d, 4H, $J = 4.0$), 4.51 (t, 2H, $J = 3.9$), 7.21–7.26 (m, 4H), 7.29–7.40 (m, 16H); ^{13}C NMR (100 MHz, CD_3OD) δ 26.5, 27.1, 27.6, 28.8, 30.3, 30.6, 33.7, 45.7, 48.0, 52.9, 128.6, 129.1, 130.2, 141.7; MS (ESI^+) *m*/*z* 760 $(M + H)^+$.

3.2. Cell culture, treatments, and data analysis

HeLa, HT29, LOVO, Saos-2, and U2OS cells were cultured in EMEM containing 10% fetal bovine serum, 1% glutamine, 1% non-essential amino acids, 1 mM pyruvate, and antibiotics. HL60 and SH-SY5Y cells [14], and human chondrocytes C-28/I2 [39] were cultured as previously described. Primary coltures of rat thymocytes were prepared as reported [40]. All cells types were routinely maintained at 37 °C in a humidified atmosphere containing 5% CO_2. All tested compounds were dissolved in DMSO and added to cell cultures (0.1% with respect to the total volume) in order to obtain the required concentration in the medium. Control cells received the corresponding volume of DMSO.

The presented experiments were performed at least three times. The results are expressed as means ± S.E.M. for the data obtained in the indicated numbers of independent experiments. In each experiment every point was done in duplicate and every point was assayed in duplicate. In some cases, results obtained in one representative experiment are shown. When statistical analysis was applicable, data were compared by Student *t*-test. Differences were considered significant for $P < 0.05$. Data analysis was performed by the GraphPad Prism 5 software.

3.3. Peroxide levels and mitochondrial membrane potential

Mitochondrial membrane potential ($\Delta\Psi m$) and intracellular peroxide levels were measured in the whole cells by fluorescent probes as described [41]. Fluorescence was analyzed by flow cytometry with logarithmic amplification. Flow cytometric analysis was performed with a Beckmann Coulter Epics XL MCL cytometer (USA) equipped with a 15 mW argon ion laser. To measure $\Delta\Psi m$, mitochondria in intact cells were probed with the potential-sensitive dye DiOC6. After the treatment, cells were incubated with medium containing 4 nM DiOC6 for 40 min at a cell concentration of 1×10^6 cell/mL at 37 °C in the dark. Cells were counterstained by propidium iodide at 5 μg/mL to eliminate dead cells. In order to detect intracellular peroxides, the cells were incubated with 5 μM DCFDA (Molecular Probes, Leiden, The Netherlands) for 30 min at 37 °C.

3.4. RNA interference

The siRNA directed against human Atg5 (SignalSilence Atg5 siRNA I) was obtained from Cell Signaling Technology. Control siRNA-A was purchased from Santa Cruz Biotechnology. For the transfection [42], cells at 50% of confluence were transfected with a final concentration of 100 nM siRNA duplex for 24 h by Transfection reagent (Santa Cruz) according to manufacturer's instructions. After further 24 h, the cells were treated with the designated compounds.

3.5. Cytotoxicity, cell death and apoptosis

Cytotoxicity was evaluated by determining cell viability by trypan blue exclusion. Samples were done in triplicate, and at least 10 fields were counted for each sample. Cell survival was calculated as the percentage of viable cells in treated samples in respect to the number of viable cells in control samples. The IC_{50} value is the concentration of toxic compound required to reduce cell survival to 50%: to determine this value, a dose–response curve was plotted and concentrations that yielded 50% survival were calculated.

The assays used to detect apoptosis were caspase activation and nuclear morphology as previously described [14]. DENSPM was provided by Tocris (Bristol, UK).

3.6. Autophagy

For TEM detection of autophagy, HeLa cells were seeded on glass slides at 1.3×10^6 cells/well for 24 h. After the treatment the cells were fixed in 2.5% glutaraldehyde in 0.1 M phosphate buffer for 2 h at 4 °C and post-fixed in 1% OsO_4 in 0.1 M phosphate buffer for 1 h at 4 °C. Subsequently, samples were dehydrated in a graded series of ethanol and embedded in Epon resin (Sigma Aldrich). Ultrathin sections were counterstained with uranyl acetate and lead citrate and observed under a Philips CM10 and digitally captured by SIS Megaview III CCD camera (FEI Company, Eindhoven, The Netherlands).

AO staining of HeLa cells was performed as described by Karna et al. [43]; images were captured with the IX50 Olympus microscope. The processing of LC3 protein was assessed by Western blotting; 50 μg of protein were processed as described by Passariello et al. [44]. Monoclonal antibody against LC3-I and LC3-II forms of the protein was from Cell Signaling Technology, Danvers, MA.

Acknowledgments

We thank the Centro Interdipartimentale Ricerche Biotecnologiche (CIRB) of the University of Bologna for the flow cytometric facility. This research was supported by grants from MIUR, Rome (PRIN projects), and by the University of Bologna (RFO funding).

References

[1] R.A. Casero Jr., P.M. Woster, Recent advances in the development of polyamine analogues as antitumor agents, J. Med. Chem. 52 (2009) 4551–4573.
[2] A.E. Pegg, Mammalian polyamine metabolism and function, IUBMB Life 61 (2009) 880–894.
[3] K. Igarashi, K. Kashiwagi, Modulation of cellular function by polyamines, Int. J. Biochem. Cell Biol. 42 (2010) 39–51.
[4] F. Madeo, T. Eisenberg, S. Büttner, C. Ruckenstuhl, G. Kroemer, Spermidine: a novel autophagy inducer and longevity elixir, Autophagy 6 (2010) 160–162.
[5] E.W. Gerner, F.L. Meyskens Jr., Polyamines and cancer: old molecules, new understanding, Nat. Rev. Cancer 4 (2004) 781–792.
[6] R.A. Casero Jr., L.J. Marton, Targeting polyamine metabolism and function in cancer and other hyperproliferative diseases, Nat. Rev. Drug Discov. 6 (2007) 6373–6390.
[7] H.M. Wallace, K. Niiranen, Polyamine analogues – an update, Amino Acids 33 (2007) 261–265.
[8] S.K. Sharma, S. Hazeldine, M.L. Crowley, A. Hanson, R. Beattie, S. Varghese, T.M. Senanayake, A. Hirata, F. Hirata, Y. Huang, Y. Wu, N. Steinbergs, T. Murray-Stewart, I. Bytheway, R.A. Casero Jr., P.M. Woster, Polyamine-based small molecule epigenetic modulators, MedChemComm 3 (2012) 14–21.
[9] M.L. Bolognesi, A. Minarini, R. Budriesi, S. Cacciaguerra, A. Chiarini, S. Spampinato, V. Tumiatti, C. Melchiorre, Universal template approach to drug design: polyamines as selective muscarinic receptor antagonists, J. Med. Chem. 41 (1998) 4150–4160.
[10] C. Melchiorre, A. Antonello, R. Banzi, M.L. Bolognesi, A. Minarini, M. Rosini, V. Tumiatti, Polymethylene tetraamine backbone as template for the development of biologically active polyamines, Med. Res. Rev. 23 (2003) 200–233.
[11] C. Melchiorre, M.L. Bolognesi, A. Minarini, M. Rosini, V. Tumiatti, Polyamines in drug discovery: from the universal template approach to the multitarget-directed ligand design strategy, J. Med. Chem. 53 (2010) 5906–5914.
[12] A. Minarini, A. Milelli, V. Tumiatti, M. Rosini, M.L. Bolognesi, C. Melchiorre, Synthetic polyamines: an overview of their multiple biological activities, Amino Acids 38 (2010) 383–392.
[13] C. Melchiorre, A. Minarini, P. Angeli, D. Giardinà, U. Gulini, W. Quaglia, Polymethylene tetraamines as muscarinic receptor probes, Trends Pharmacol. Sci. 10 (1989) 55–59.
[14] M. Zini, C.L. Passariello, D. Gottardi, S. Cetrullo, F. Flamigni, C. Pignatti, A. Minarini, V. Tumiatti, A. Milelli, C. Melchiorre, C. Stefanelli, Cytotoxicity of methoctramine and methoctramine-related polyamines, Chem. Biol. Interact. 181 (2009) 409–416.
[15] R. Saiki, Y. Yoshizawa, A. Minarini, A. Milelli, C. Marchetti, V. Tumiatti, T. Toida, K. Kashiwagi, K. Igarashi, In vitro and in vivo evaluation of polymethylene tetraamine derivatives as NMDA receptor channel blockers, Bioorg. Med. Chem. Lett. 23 (2013) 3901–3904.
[16] C. Melchiorre, A. Minarini, W. Quaglia, V. Tumiatti, Methoctramine, Drug Future 14 (1989) 628–631.
[17] A. Minarini, R. Budriesi, A. Chiarini, C. Melchiorre, V. Tumiatti, Further investigation on methoctramine-related tetraamines: effects of terminal *N*-substitution and of chain length separating the four nitrogens on M2 muscarinic receptor blocking activity, Farmaco 46 (1991) 1167–1178.
[18] V. Tumiatti, V. Andrisano, R. Banzi, M. Bartolini, A. Minarini, M. Rosini, C. Melchiorre, Structure–activity relationships of acetylcholinesterase non-covalent inhibitors based on a polyamine backbone. 3. Effect of replacing the inner polymethylene chain with cyclic moieties, J. Med. Chem. 47 (2004) 6490–6498.
[19] V. Tumiatti, A. Minarini, A. Milelli, M. Rosini, M. Buccioni, G. Marucci, C. Ghelardini, C. Bellucci, C. Melchiorre, Structure–activity relationships of methoctramine-related polyamines as muscarinic antagonist: effect of replacing the inner polymethylene chain with cyclic moieties, Bioorg. Med. Chem. 15 (2007) 2312–2321.
[20] Y. Chen, D.L. Kramer, P. Diegelman, S. Vujcic, C.W. Porter, Apoptotic signaling in polyamine analogue-treated SK-MEL-28 human melanoma cells, Cancer Res. 61 (2001) 6437–6444.
[21] L. Yang, J. Zhao, Y. Zhu, Z. Tian, C. Wang, Reactive oxygen species (ROS) accumulation induced by mononaphthalimide-spermidine leads to intrinsic and AIF-mediated apoptosis in HeLa cells, Oncol. Rep. 25 (2011) 1099–1107.
[22] A. Milelli, V. Tumiatti, M. Micco, M. Rosini, G. Zuccari, L. Raffaghello, G. Bianchi, V. Pistoia, J. Fernando Díaz, B. Pera, C. Trigili, I. Barasoain, C. Musetti, M. Toniolo, C. Sissi, S. Alcaro, F. Moraca, M. Zini, C. Stefanelli, A. Minarini, Structure–activity relationships of novel substituted naphthalene diimides as anticancer agents, Eur. J. Med. Chem. 57 (2012) 417–428.
[23] A.J. Palmer, H.M. Wallace, The polyamine transport system as a target for anticancer drug development, Amino Acids 38 (2010) 415–422.
[24] R.H. Davis, J.L. Ristow, Uptake, intracellular binding, and excretion of polyamine during growth of Neurospora crassa, Arch. Biochem. Biophys. 271 (1989) 315–322.
[25] D. Soulet, L. Covassin, M. Kaouass, R. Charest-Gaudreault, M. Audette, R. Poulin, Role of endocytosis in the internalization of spermidine-C(2)-BODIPY, a highly fluorescent probe of polyamine transport, Biochem. J. 367 (2002) 347–357.

[26] I.N. Lavrik, A. Golks, P.H. Krammer, Caspases: pharmacological manipulation of cell death, J. Clin. Invest. 115 (2005) 2665–2672.
[27] J.D. Robertson, S. Orrenius, B. Zhivotovsky, Nuclear events in apoptosis, J. Struct. Biol. 129 (2000) 346–358.
[28] J.S. Long, K.M. Ryan, New frontiers in promoting tumour cell death: targeting apoptosis, necroptosis and autophagy, Oncogene 31 (2012) 5045–5060.
[29] A. Notte, L. Leclere, C. Michiels, Autophagy as a mediator of chemotherapy-induced cell death in cancer, Biochem. Pharmacol. 82 (2011) 427–434.
[30] S. Zhou, L. Zhao, M. Kuang, B. Zhang, Z. Liang, T. Yi, Y. Wei, X. Zhao, Autophagy in tumorigenesis and cancer therapy: Dr. Jekyll or Mr. Hyde? Cancer Lett. 23 (2012) 115–127.
[31] T. Eisenberg, H. Knauer, A. Schauer, S. Büttner, C. Ruckenstuhl, D. Carmona-Gutierrez, J. Ring, S. Schroeder, C. Magnes, L. Antonacci, H. Fussi, L. Deszcz, R. Hartl, E. Schraml, A. Criollo, E. Megalou, D. Weiskopf, P. Laun, G. Heeren, M. Breitenbach, B. Grubeck-Loebenstein, E. Herker, B. Fahrenkrog, K.U. Fröhlich, F. Sinner, N. Tavernarakis, N. Minois, G. Kroemer, F. Madeo, Induction of autophagy by spermidine promotes longevity, Nat. Cell. Biol. 11 (2009) 1305–1314.
[32] Y. Kabeya, N. Mizushima, T. Ueno, A. Yamamoto, T. Kirisako, T. Noda, E. Kominami, Y. Ohsumi, T. Yoshimori, LC3, a mammalian homologue of yeast Apg8p, is localized in autophagosome membranes after processing, EMBO J. 19 (2000) 5720–5728.
[33] S. Shen, O. Kepp, G. Kroemer, The end of autophagic cell death? Autophagy 8 (2012) 1–3.
[34] R.G. Carroll, S.J. Martin, Autophagy in multiple myeloma: what makes you stronger can also kill you, Cancer Cell 23 (2013) 425–426.
[35] S. Yousefi, H.U. Simon, Apoptosis regulation by autophagy gene 5, Crit. Rev. Oncol. Hematol. 63 (2007) 241–244.
[36] C. Stefanelli, F. Bonavita, I. Stanic', M. Mignani, A. Facchini, C. Pignatti, F. Flamigni, C.M. Caldarera, Spermine causes caspase activation in leukaemia cells, FEBS Lett. 437 (1998) 233–236.
[37] S.Q. Xie, Q. Li, Y.H. Zhang, J.H. Wang, Z.H. Mei, J. Zhao, C.J. Wang, NPC-16, a novel naphthalimide-polyamine conjugate, induced apoptosis and autophagy in human hepatoma HepG2 cells and Bel-7402 cells, Apoptosis 16 (2011) 27–34.
[38] A.M. Choi, S.W. Ryter, B. Levine, Autophagy in human health and disease, N. Engl. J. Med. 368 (2013) 651–662.
[39] I. Stanic, A. Facchini, R.M. Borzì, R. Vitellozzi, C. Stefanelli, M.B. Goldring, C. Guarnieri, A. Facchini, F. Flamigni, Polyamine depletion inhibits apoptosis following blocking of survival pathways in human chondrocytes stimulated by tumor necrosis factor-alpha, J. Cell. Physiol. 206 (2006) 138–146.
[40] C. Stefanelli, F. Bonavita, I. Stanic', G. Farruggia, E. Falcieri, I. Robuffo, C. Pignatti, C. Muscari, C. Rossoni, C. Guarnieri, C.M. Caldarera, ATP depletion inhibits glucocorticoid-induced thymocyte apoptosis, Biochem. J. 322 (1997) 909–917.
[41] A. Andreani, S. Burnelli, M. Granaiola, A. Leoni, A. Locatelli, R. Morigi, M. Rambaldi, L. Varoli, N. Calonghi, C. Cappadone, G. Farruggia, M. Zini, C. Stefanelli, L. Masotti, N.S. Radin, R.H. Shoemaker, New antitumor imidazo [2,1-b]thiazole guanylhydrazones and analogues, J. Med. Chem. 51 (2008) 809–816.
[42] C.L. Passariello, M. Zini, P.A. Nassi, C. Pignatti, C. Stefanelli, Upregulation of SIRT1 deacetylase in phenylephrine-treated cardiomyoblasts, Biochem. Biophys. Res. Commun. 407 (2011) 512–516.
[43] P. Karna, S. Zughaier, V. Pannu, R. Simmons, S. Narayan, R. Aneja, Induction of reactive oxygen species-mediated autophagy by a novel microtubule-modulating agent, J. Biol. Chem. 285 (2010) 18737–18748.
[44] C.L. Passariello, D. Gottardi, S. Cetrullo, M. Zini, G. Campana, B. Tantini, C. Pignatti, F. Flamigni, C. Guarnieri, C.M. Caldarera, C. Stefanelli, Evidence that AMP-activated protein kinase can negatively modulate ornithine decarboxylase activity in cardiac myoblasts, Biochim. Biophys. Acta 1823 (2012) 800–807.